Can combination of UAV-derived vegetation indices with biophysical variable(s) improve yield variability assessment in smallholder farms?

Authors: Julius B. Adewopo[1], Helen Peter[1], Ibrahim Mohammed[1], Peter Craufurd[2], Alpha Kamara[1], Bernard Vanlauwe[3]

Corresponding author: Julius Adewopo, j.adewopo@cgiar.org

Affiliations:
[1]International Institute for Tropical Agriculture – IITA, Kano Research Station, Kano, Nigeria.
[2] International Center for Maize and Wheat Improvement – CIMMYT, Nairobi, Kenya.
[3] International Institute for Tropical Agriculture – IITA, Central Africa Hub, Duduville, Nairobi, Kenya.

Abstract:
Rapid assessment of maize yields in smallholder farming system is important to understand its spatial and temporal variability and for timely agronomic decision-support. Imageries acquired with unmanned air vehicles (UAV) offer opportunity to assess agronomic variables at field scale, however, it is not clear if this can be translated into reliable yield assessment on smallholder farms where field conditions, maize genotypes, and management practices vary within short distances. This study was conducted to assess the predictability of maize grain yield using UAV-derived vegetation indices (VI), with(out) biophysical variables, in smallholder farms. High-resolution images were acquired with UAV-borne multispectral sensor at 4 and 8 weeks after sowing (WAS) on 31 farmers' managed fields (FMFs) and 12 nearby Nutrient Omission Trials (NOT), all distributed across 5 locations within the core maize region of Nigeria. The NOTs included non-fertilized and fertilized plots (with and without micronutrients), sown with open pollinated or hybrid maize genotypes. Acquired multispectral images were post-processed into several three (s) vegetation indices (VIs), normalized difference vegetation index (NDVI), normalized difference red-edge (NDRE), green-normalized difference vegetation index (GNDVI). Biophysical variables, plant height (Ht) and percent canopy cover (CC), were measured with the georeferenced plot locations recorded. In the NOTs, the nutrient status, not genotype, influenced the grain yield variability and outcome. The maximum grain yield observed in NOTs was 9.3 tha^{-1}, compared to 5.4 tha^{-1} in FMF. Without accounting for between- and within-field variations, there was no relationship between UAV-derived VIs and grain yield at 4WAS ($r<0.02$, $P>0.1$), but significant correlations were observed at 8WAS ($r\leq0.3$; $p<0.001$). Ht was positively correlated with grain yield at 4WAS ($r=0.5$, $R^2=0.25$, $p<0.001$), and more strongly at 8WAS ($r=0.7$, $R^2=0.55$, $p<0.001$), while relationship between CC and yield was only significant at 8WAS. By accounting for within- and between-field variations in NOTs and FMF (separately) through linear mixed effects modeling, predictability of grain yield from UAV-derived VIs was generally ($R^2\leq0.24$), however, the inclusion of ground-measured biophysical variable (mainly Ht) improved the explained yield variability ($R^2 \geq0.62$, $RMSEP\leq0.35$) in NOTs but not in FMF. We conclude that yield prediction with UAV-acquired imageries (before harvest) is more reliable under controlled experimental conditions (NOTs), compared to actual farmer managed fields where various confounding agronomic factors can amplify noise-signal ratio.

Keywords: UAV; multi-spectral imageries; multi-locational, Maize yield; smallholder; vegetation indices

Introduction

Assessment of crop yield at scale is needed to quantify and address productivity gaps (Burke and Lobell, 2017; Titonnell *et al.*, 2005), yet associated costs are limiting for robust sampling at scale. Hence, the development of appropriate technologies and methods that can provide leverage for quick and non-destructive data collection remains a priority. The emergence and evolution of remote-sensing technologies for the acquisition and processing of remotely-sensed proxy data is potentially valuable for the assessment of yield or other agronomic variables at various scales. However, this is limited by associated costs and availability of quality images for in-season and out-of-season applications. Smallholder farming systems of sub-Saharan Africa (SSA) are often characterized by fragmented farmlands and differentiated management practices (Herbert, 2005; Giller *et al.,* 2011; Onuk *et al.*, 2015; Vanlauwe, *et al.,* 2015). Most landscapes are complex mosaics with diffuse field boundaries and trees. Therefore, imagery of the landscape needs to have sufficient spatial and temporal resolution to mask out artefacts of vegetation or undesired features. Spatially-explicit data acquired over farming landscapes can improve the understanding of the variability and dynamics of agronomic processes and variables, especially in smallholder cropping systems where changes may be more frequent at smaller scales. Quite often, these changes are influenced by management preferences of the farmers whose decisions are mostly driven by various external factors, including accessibility and affordability of inputs (Nagy and Edun, 2002; Olarinde *et al.,* 2007). At the minimum, smallholder farming landscapes are defined by different varieties sown at different with different soil nutrient application or status. Consequently, smallholder farming landscapes are often characterized as mosaic(s) of individual fields which have contrasting vegetation structures or types within a very small area (often, within tens of meters). It is uncertain if and how such complexities can be harnessed to optimize yields, by rapidly assessing in-season variability and diagnose within-field constraints such as nutrient limitations.

The recent advances in satellite-based remote-sensing of global land-cover coincides with the emergence of Unmanned aerial/air vehicles (UAVs) for crop monitoring and yield assessment, therefore adoption of UAV is expected to spread across large-scale mono-cropped and smallholder multi-cropped farming systems (Efron, 2015; Hall, 2016; Yang, 2017). UAVs were initially developed for military use but have become recognized as a tool to acquire high-resolution images that can be [post]-processed and analyzed to understand spatially varying agronomic factors at field scale. Within the past five years, several researchers have reported on the applicability of UAV for monitoring agronomic variables, (e.g., Benincasa *et al.*, 2017, Yang *et al.,* 2017; Zhang *et al.*, 2014) in different cropping systems and across diverse geographies (Hall, 2016; Song, 2016; Nebiker *et al.*, 2016, Salami *et al.*, 2014;). Many of these variables are considered as potential proxies for yield estimation (Hall, 2016; Song, 2016; Nebiker *et al.*, 2016), especially at the plot and field level (typically up to 1000ha). There are several existing methods for estimating crop yields with remote-sensing. A popular approach is to relate measured location-specific yield to vegetation indices derived from RGB, multi-spectral, or hyper spectral camera sensors. Vegetation indices respond often provide strong expression of the ground cover and chlorophyll content of green material (Tucker, 1979; Huete *et al.,* 2002). Many vegetation indices (VIs) have been developed, with the most common being the normalized difference vegetation index – NDVI (Hall, 2016; Haghighattalab *et al.,* 2015; Maresma *et al.,* 2016; Vega *et al.*, 2015; Yang, *et al.*, 2017). Based on varied relationships between different reflectance spectral bands, other relevant VIs have been applied in diverse agricultural production systems. These include the normalized difference red-edge (NDRE), green normalized difference vegetation index (GNDVI), green canopy vegetation index (GCVI), red

vegetation index (RVI), and red-edge canopy index (RECI) and many others (Gitelson *et al.*, 2011; Nguy-Robertson *et al.,* 2012). Since these VIs represent spectral (and to a lesser extent, structural) characteristics of the vegetation, they are potential proxies for rapid assessment of yield and yield variability. Further, when these VIs are derived from spatially-explicit remotely-sensed imageries, they can provide very useful understanding of yield variability, at varying spatial scales. The diagnosis of nutrient constraints and crop yield differences between fields/plots with the use of individual VIs have been promising e.g. (Benincasa *et al.,* 2017; Wahab *et al.,* 2018), and researchers have proposed that combination of VIs can provide additive sensitivity effect and improve the detectability of nuanced vegetational characteristics to improve the assessment of variations in agronomic parameters, including yield (e.g. Gitelson *et al.*, 2011; Nguy-Robertson *et al.,* 2012). This is because single VIs can be constrained by vegetation structure and composition which may be undetectable at specific wavelengths of the electromagnetic spectrum. For instance, greenness of plants grown under adequate nutrient conditions has been reported to compromise the accuracy of the remotely-sensed NDVI by multispectral sensor due to saturation within the green spectral band (Isla *et al.*, 2011; Gu *et al.*, 2013; Maresma *et al.* 2016). This type of limitation can be avoided by using other VIs which relies on spectral information from other reflectance bands within the electromagnetic spectrum.

While agronomic applications of UAVs are fast evolving (Yang *et al.*, 2017), there are limitations. For instance, Watanabe *et al.* (2017) indicated that sorghum plant height was overestimated by UAV, and that high fertilization affected the relationship between UAV and ground-based measurements. Schut *et al.* (2018) reported that vegetation indices did not capture all management and biophysical factors that can aid the accurate assessment of yield within fields. Yet, new generation UAV-borne sensors may offer improved assessment accuracies for crop monitoring especially in combination with [few] ground level data. According to Sibley *et al.,* (2013) and Schut *et al.* (2018), repeated in-season measurements and good field-level accuracy are important criteria to derive useful information from remotely-sensed imageries for rapid yield (and other agronomic) assessments. Given the complexity of smallholder farming systems (Titonnell *et al.*, 2005; Vanlauwe *et al.,* 2015), it is important to assess the field applicability of UAV, beyond experimental plot conditions, and within actual complex farming landscapes where they can be deployed for rapid farm-level decision support. Schut *et al.* (2018) indicated yield variability explained by selected VIs within specific crop farms reduced greatly across an array of fields compared to within fields where there is a higher homogeneity and noted that accurate ground reference data may improve the assessment of in-season yield variability. These ground data can include biophysical variables, such as plant height (Ht) and Canopy Cover (CC), which have been reported as valuable for non-destructive yield(-variability) assessment in smallholder farmers' field. These biophysical variables represent morphological characteristics and are useful for understanding allometric characteristics of plants (Tittonell *et al.*, 2005). There is a major knowledge gap regarding the potential to improve in-season assessment of maize yield(-variability) in farmers field through combination of ground-measured biophysical variables with UAV-derived VIs. Yet, there is a critical need to evolve reliable and rapid approaches for timely decision support within smallholder farming systems. Therefore, we conducted this study, within the maize-producing savanna region of Nigeria, to assess in-season predictability of grain yield in multilocational smallholder maize farmers' fields using UAV-derived VI with and without ancillary observations of biophysical variables.

Preprints (www.preprints.org) | NOT PEER-REVIEWED | Posted: 13 October 2020 doi:10.20944/preprints202010.0264.v1

Material and methods

2.1 Study Area

This study was carried out at multiple locations within the core maize production region of Nigeria, namely Bunkure, Doguwa, Funtua, Ikara, and Soba (Figure 1). The locations are within the Sudan and Northern Guinea savanna agroecologies of the Country, which is the major cropping regions for grains and legumes such as maize (*Zea mays*), cowpea (*Vigna unguiculata*), peanut (*Arachis hypogaea*), and soybeans (*Glycine max*). The target areas for UAV-based data collection were selected based on: (i) the location of nutrient omission trials (NOT) which were established under a different research activity to identify and understand nutrient constraints that are limiting maize yield among smallholder maize farmers (Shehu *et al.,* 2018); (ii) the willingness of proximal farmers to grant access for ground-truthing and yield assessment in their farms, and (iii) the advisory guidance of National Space Research and Development Agency (NASRDA) in Nigeria, which is critical for compliance with regulatory requirements on UAV use in the Country.

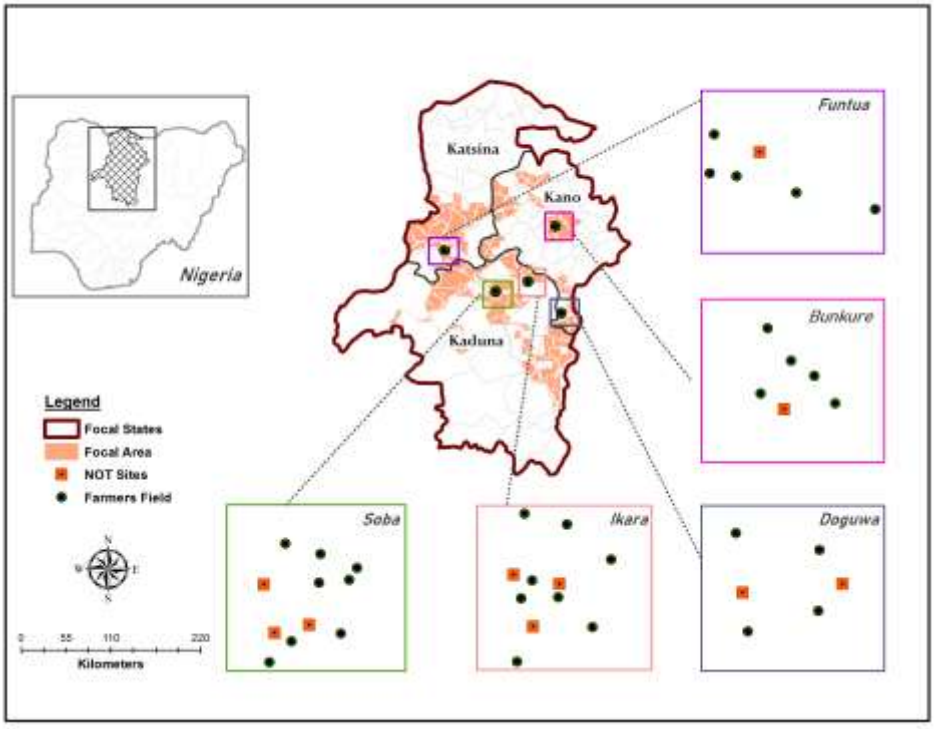

Figure 1: Map showing the multi-location of the farmers' field and nutrient omission trials (NOT) that were covered by unmanned air vehicle (UAV) flight missions and included in this study.

Preprints (www.preprints.org) | NOT PEER-REVIEWED | Posted: 13 October 2020 doi:10.20944/preprints202010.0264.v1

2.2 Smallholder Farmers' Fields and Nutrient Omission Trials (NOT)

2.2.1 Nutrient Omission Trial Field (NOT) establishment: At the onset of the planting season for the region, mid to late June 2016, NOTs (n=100) were established to assess the impact of varying soil nutrient limitations on maize yield within the maize-based system of Nigeria under the Taking Maize Agronomy to Scale in Africa (TAMASA) project (www.tamasa.cimmyt.org; Shehu *et al.,* 2018). A subset of the NOTs (n=12) were covered within the target locations for UAV flight. Each experimental unit comprised of 12 contiguous plots (5.2m x 4m) planted with maize in two blocks of six plots, with one block sown with open-pollinated genotype (OPV) and the other sown with hybrid genotype (HV). Within each of the genotype block, nutrient omission fertilizer treatments were applied at recommended optimal dosage, based on previous soil tests in the region. The nutrient treatments comprised a combination of major nutrients required for maize production, including nitrogen (N), phosphorus (P), potassium (K) and micronutrients (+). Hence, each genotype block received six fertilizer treatments (i.e. Control, PK, NP, NK, NPK, and NPK+) applied on six plots, across twelve (12) multi-locational NOTs. Therefore, a total of 144 plots were covered during flight missions at 4WAS and 8 WAS, across all the target locations. All nutrients were applied at the establishment stage of NOT, except N which was applied in 3 splits (at establishment, 3 WAS, and 6 WAS). Other details on rates and management of NOTs are presented by Shehu *et al.* (2018).

2.2.2 Farmers' fields: Since farmers made their farm-level decisions independent of our research interests, we screened prospective volunteer farmers to select only farmlands that were sown with maize within about 3 days of NOT establishment. The selected farmers' fields (n=32) differed in size and management, a typical configuration within smallholder maize-based systems. The specific varietal choice of the farmers is generally unknown, however, within the maize-based area, farmers sow both the open-pollinated (OPV) and hybrid (HV) genotypes.

2.3 UAV-based Imagery Acquisition and post-processing

We used an eBee UAV (SenseFly Inc., Switzerland, www.sensefly.com/drone/ebee.html) mounted with multispectral 4C sensor (Airinov, France, www.airinov.fr) to acquire fine resolution images at each target location. The e-Bee is a light-weight fixed-wing UAV, which can cover up to 600ha in a single flight at 1000m altitude, equipped with an onboard global positioning system (GPS), solar irradiance sensor, and a ground calibration target. The multi-spec 4C camera has four passive sensors that record reflectance in four spectral bands - red (R), green (G), red-edge (RE), and near infra-red (NIR) at 1.2 megapixels per sensor. It has a global shutter, instant field of view (IFOV) of 0.9mrad, and low luminosity (>3000lux). The UAV was flown to acquire fine-resolution images that cover the area of interest (including NOT and farmers' fields) at 4 and 8 WAS, coinciding with the onset of vegetative (V7) and tasseling (VT) growth stages, respectively (Ritchie *et al.*, 1993), and within the mid-season growth period where best indication of post-harvest grain yield is obtainable (Geipel *et al.* 2014).

2.3.4 Post-processing

After the completion of each flight mission, the imageries were exported from the UAV along with the flight log files for post-processing with Pix4D software (Pix4D v.3.1., Switzerland, www.pix4d.com). The software provided platform for end-to-end post-processing of acquired imageries and offers the needed flexibility to configure processing parameters based on desired output quality and target end-use of the products. Overall, for each successful flight mission, ~ 400 images were geotagged and processed

Preprints (www.preprints.org) | NOT PEER-REVIEWED | Posted: 13 October 2020 doi:10.20944/preprints202010.0264.v1

through several stages to generate final outputs in geotiff formats, including reflectance bands corresponding to the four spectral reflectance domains of the multi-spec sensor, digital surface model, digital orthomosaics, and VIs. The VI imageries were computed from corresponding spectral bands, based on Equations i-iii. The consideration of VIs to be computed was limited to those that have been reported as promising for agronomic application at the canopy level and in relation to vegetation status in croplands, especially maize, with focus on selecting VIs are based on red, red-edge, and green bands (Cammarano *et al.*, 2014; Gitelson *et al.,* 2005; Hatfield and Prueger, 2010; Vina *et al*., 2011; Xue and Su, 2017)

$$NDVI = \frac{\rho nir - \rho red}{\rho nir + \rho red} \quad \text{(i)}$$

$$NDRE = \frac{\rho nir - \rho red.edge}{\rho nir + \rho red.edge} \quad \text{(ii)}$$

$$GNDVI = \frac{\rho nir - \rho green}{\rho nir + \rho green} \quad \text{(iii)}$$

Where, $\rho nir, \rho red, \rho red.edge, and\ \rho green$ are the spectral reflectance of the near infrared band, red band, red edge band, and green band, respectively.

2.4 Ground-truth data collection

We conducted in-situ measurement of NDVI with Greenseeker Handheld Crop Sensor HCS 100 (Trimble Ltd., Sunnyvale, CA; https://agriculture.trimble.com/precision-ag/products/greenseeker). The Greenseeker was held above the canopy (0.6 m) while walking for 30 - 60 seconds through each NOT plot, or marked quadrats ($4m^2$, n = 5) within each farm. The device proximally scans leaf greenness (within a swath of ~0.25 m) through its infrared sensors and displays an NDVI value averaged over duration of the scan. We did not acquire ground-truth measurement for other VIs due to cost (money and labor) and because our goal was not to recalibrate the sensor, but rather to test the application of UAV-borne multispectral sensor, for assessing yield variability based on the indices derived.

We adopted the crop-cut method to quantify grain yield, as recommended by the FAO and generally regarded as the most objective method for yield estimation (Carletto *et al.,* 2015; Wahab *et al.* 2018). Harvest was conducted within $9m^2$ quadrats in each NOT treatment plot, based on standard NOT protocols, as presented by Nziguheba *et al.* (2009). In farmer' fields, maize cobs were harvested and grain yield was quantified in five (2m x2m) quadrats positioned along a diagonal transect within the field. In both farmers' fields and NOTs, the harvested cobs were shelled, and grain was oven dried to determine moisture content. The weight of grain yield per sampling quadrat were converted to yields in metric tons per hectare (t/ha) at 12% moisture content. The geographic coordinates were recorded as degrees latitude and longitude at the center of each plot/quadrat in NOT and farmers' field using a

Preprints (www.preprints.org) | NOT PEER-REVIEWED | Posted: 13 October 2020 doi:10.20944/preprints202010.0264.v1

Garmin eTrex 20 GPS device (https://buy.garmin.com/en-US/US/p/87771#overview). Using Height ruler, we measured height of 3 randomly selected maize stands within each quadrat, and the recorded values were later averaged per quadrat at 4WAS and 8WAS. Similarly, at both growth stages, we used smartphone-based Canopeo app (http://canopeoapp.com/) to measure percent canopy cover in each quadrat, based on standard protocols (Patrignani and Ochsner, 2015).

2.5 Data Analyses

Data cleaning and multi-step spatial analyses of the data collected through ground measurements and UAV-derived datasets were conducted using ArcGIS 10.3.1 (ESRI, Redlands, California, http://www.esri.com/arcgis/about-arcgis) and open-source packages (including RGDAL, LMER, and GGPLOT) in R analytical platform v.3.4.1.

2.5.1 Georeferenced locations and Data Extraction

The recorded geographic coordinates (X,Y) were processed and exported into point shapefiles in WGS1984 datum in ArcMap. Using the UAV-derived imagery as a reference, some misaligned coordinates were noted and corrected by editing the point shapefiles in ArcGIS. These misalignments are likely due to the precision level of the recreational GPS unit (~4m), hence, the editing process was critical to ensure that each point shapefile location rests within designated field, and references the appropriate NOT plot or farmers' field. Using the geoprocessing "Create Regular Polygon" add-on tool in ArcGIS, 4-sided polygons ($2m^2$ for farmers' field and $3m^2$ for NOTs) were generated for each ground-truthing points, using the point datasets as the centroid. These polygons represent the sampling support unit for the ground-truthing process and were subsequently used in R (Raster package, Hijmans *et al.,* 2016), to compute zonal average statistics of UAV-derived VI cell values, for each location at the matching support scale of the yield measurements.

2.5.2 Statistical Analyses of Data

Due to the slight skewness of the yield data, we applied log-linear transformation to normalize the dataset. The output from the spatial zonal statistics which was computed from the UAV-derived imageries, was processed as table and imported into R-Studio to assess correlation of VIs with measured grain yield across the study locations, and separately within NOTs and FMFs. In the first level of the analyses, we used linear multivariate regression approach (Equa. iv) to assess the variability of yield that is explained by ground-measured variables in NOTs.

$$yield_i = \beta_0 + \beta_1 X_1 + \beta_2 X_2 + \beta_i X_i + \varepsilon_{ij} \quad \text{iv.}$$

Where, β_0 is the intercept, $\beta_{1,2,i}$ are slopes of observed variables X_1, X_2, X_i, respectively.

In the second level, we independently and randomly split the NOT and FMF data into 70% calibration data (93 datapoints for NOT and 72 data points for FMF) and 30% validation data (37 datapoints for NOT and 27 data points for FMF). Some data records were excluded from further analyses in NOTs and FMFs due to irresolvable missing datapoints or incomplete records. The random split of each dataset was implemented at the Farm (i.e. field) level for independence of locations in the model calibration and validation stages. Notwithstanding the assumption that both NOT and FMF data accrue to the same population (i.e. smallholder farmers), separate models were fitted for NOTs vs. FMFs. The calibration

Preprints (www.preprints.org) | NOT PEER-REVIEWED | Posted: 13 October 2020 doi:10.20944/preprints202010.0264.v1

datasets were used to fit linear mixed effect models (Equa. v) for yield prediction, using UAV-derived VIs at 4WAS and 8WAS as input variables, with and without the significant biophysical variables (as determined from first step). The validation datasets were used to assess the accuracy of the prediction. Similar to Burke and Lobell (2017), model fit was also applied to time series combination of 4WAS and 8WAS data, to assess potential applicability for improved prediction outcome (Equa. vi). The linear mixed effect modeling framework included a random parameter that accounts for potential indeterminable effect of differing management practices among farmers. Statistical parameters that were evaluated to make inference include descriptive statistics (mean, range, coefficient of variation), correlation coefficient (r, Equa. vii), coefficient of determination (R^2, Equa. Viii), root means square error of prediction (RMSEP; Equa. ix) and significance, *P* (tested at 95% confidence level). The best relationship between measured yield and UAV-derived VIs is indicated by r closer to 1, R^2 closer to 1, RMSEP closer to 0, and acceptable significance level (p<=0.05).

$$yield_i = \beta_0 + \beta_1 VI_1 \dots\dots\dots + \beta_i X_i + (1|Farm) + \varepsilon_{ij} \quad \text{v.}$$

$$yield_i = \beta_0 + \sum_{t=4}^{t=8} \beta_{1t} VI_{1t} \dots\dots\dots + \sum_{t=4}^{t=8} \beta_{it} X_{it} + (1|Farm) + \varepsilon_{ij} \quad \text{vi.}$$

$$r = \frac{n(\sum_i^j (Y_{obs} * Y_{pred})) - (\sum_i^j (Y_{obs}) * \sum_i^j (Y_{pred}))}{\sqrt{(n\sum((Y_{obs})\text{^}2 - \left(\sum_i^j (Y_{obs})\right)\text{^}2) * (n\sum((Y_{pred})\text{^}2 - (\sum_i^j (Y_{pred}))\text{^}2)}} \quad \text{vii.}$$

$$R^2 = 1 - \frac{\sum_i^j (Y_{obs} - \hat{Y}_{pred})\text{^}2}{\sum_i^j (Y_{obs} - \overline{Y}_{obs})\text{^}2} \quad \text{viii.}$$

$$RMSEP = \sqrt{\frac{\sum((Y_{obs} - \hat{Y}_{pred})\text{^}2)}{n}} \quad \text{ix.}$$

Where, β_0 is the intercept, β_1 is slope of UAV-derived Vegetation Index, VI_1, β_i is the slope of measured biophysical variable X_i (when included in the model), and *t* is the growth stage at which the imageries were acquired (in weeks after sowing, WAS). The additional term, 1|Farm, denotes assignment of Farm as random variable where several factors can influence yield outcome. RMSEP is it root mean square error of prediction; Y_{obs} is the observed grain yield; $\hat{Y}_{pred}$ is the predicted grain yield; $\overline{Y}_{obs}$ is the mean of observed grain yield; *n* is the number of datapoints.

Preprints (www.preprints.org) | NOT PEER-REVIEWED | Posted: 13 October 2020 doi:10.20944/preprints202010.0264.v1

3.0 Results

3.1 Estimated grain yield and ground-truth biophysical variables (gNDVI, Ht, and CC)

The overall average estimated maize grain yield was 3.12 t/ha, with lower average yield estimated in FMF (2.75 t/ha), than the average yield across the NOT plots (3.6 t/ha; Table 1). The maximum grain yield (9.3t/ha) was attained by optimizing nutrient and genotype combination in NOT, exceeding the maximum estimated yield in farmers' fields (5.4t/ha; Fig. 2). Based on averages per treatment in NOT plots, green seeker-measured gNDVI increased from 4WAS to 8WAS, and similar results were noted for Ht and CC (Fig 3).

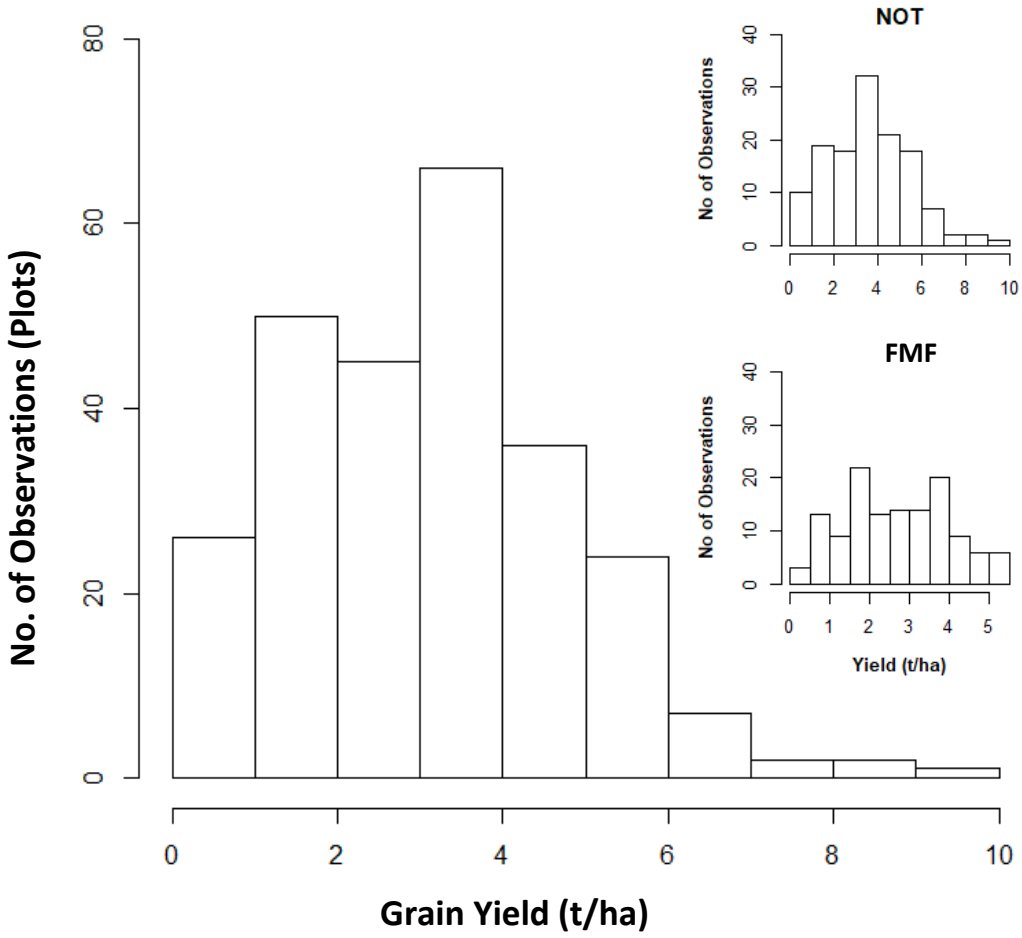

Figure 2: Observed distribution of maize grain yield as estimated in smallholder farms across multi-locational Nutrient Omission Trials (NOT) and Farmer Managed Fields (FMF).

Preprints (www.preprints.org) | NOT PEER-REVIEWED | Posted: 13 October 2020 doi:10.20944/preprints202010.0264.v1

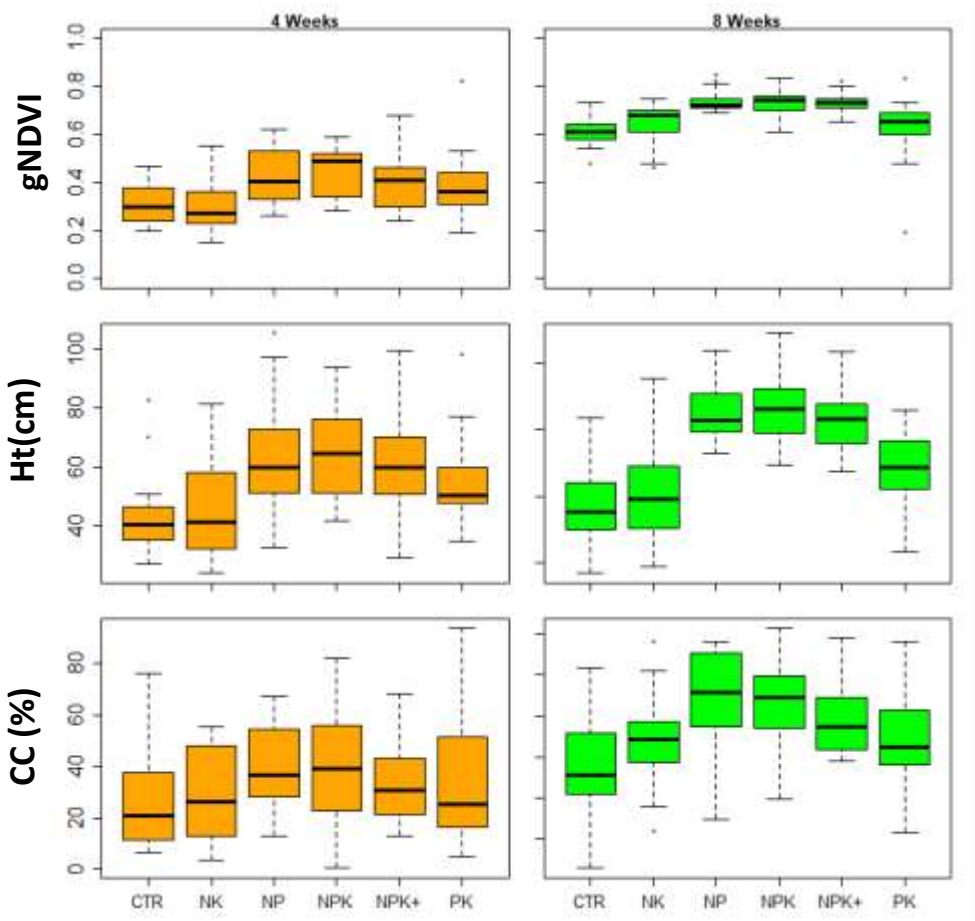

Figure 3: Ground measured normalized difference vegetation index (NDVI), plant height (Ht), and percent canopy cover (CC) of maize in smallholder farms imposed with different nutrient treatment conditions under multi-locational and widely distributed Nutrient Omission Trial (NOT).

*CTR = Control, N= Nitrogen, P = Phosphorus, K = Potassium, and + denotes addition of micronutrients.

*The horizontal line on each boxplots shows mean value and the whiskers indicate the 95% confidence interval.

304

305

Preprints (www.preprints.org) | NOT PEER-REVIEWED | Posted: 13 October 2020 doi:10.20944/preprints202010.0264.v1

306 The initial analyses of univariate relationship between grain yield and ground-measured variables
307 indicated a poor correlation (R^2<0.02; r<0.14 ; Figure 4). However, by including the known explanatory
308 variables (treatment, location, and genotype) into linear multivariate model, the explained variation in
309 yield greatly improved (R^2= 0.45 for all data, R^2=0.67 for NOT, and R^2=0.14 for FMF). Also, the
310 mutlivariate analysis of the NOT data showed that treatment and location, but not genotype,
311 significantly explained the observed yield variability (R^2= 0.50; *P<0.001)*. The average estimated yields
312 for HV (3.41 t/ha) was comparable to OPV (3.68 t/ha), considering all locations and treatments.

313

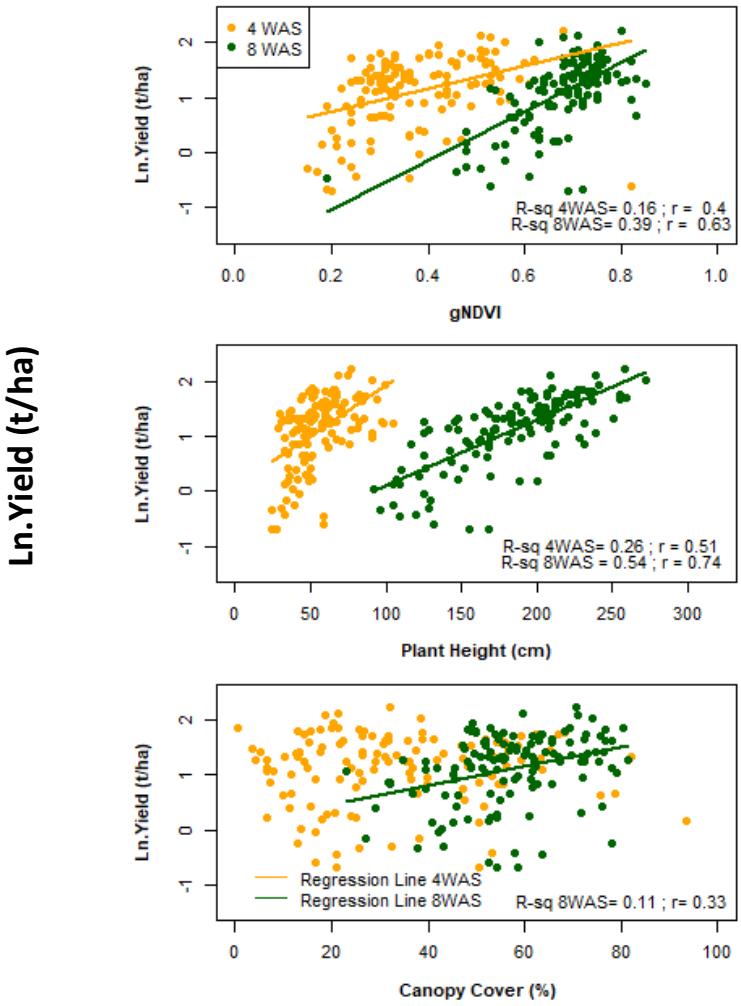

Figure 4: Univariate relationship between maize grain yield and measured normalized difference vegetation index (gNDVI), plant height, and canopy cover percentage measured on Nutrient Omission Trials (NOTs) within smallholder maize farms in Nigeria. Regression lines are included for only significant relationships, assessed by the coefficient of determination, R-sq (at α=0.05).

314

Preprints (www.preprints.org) | NOT PEER-REVIEWED | Posted: 13 October 2020 doi:10.20944/preprints202010.0264.v1

Table 1: Summary of multivariate assessment of yield variability in nutrient omission trial (NOT) plots established at multiple locations within smallholder maize-based system of Nigeria.

Growth Stage	Source of Variation	*DF*	*P-Value*	Adj. R^2
4WAS	Genotype	1	0.69	0.59***
	Treatment	5	<0.001	
	Location	4	<0.001	
	gNDVI	1	0.21	
	Ht	1	<0.001	
	CC	1	0.63	
8WAS	Genotype	1	0.67	0.64***
	Treatment	5	<0.001	
	Location	4	<0.001	
	gNDVI	1	<0.001	
	Ht	1	<0.001	
	CC	1	0.04	
4+8 WAS	Genotype	1	0.66	0.67***
	Treatment	5	<0.001	
	Location	4	<0.001	
	gNDVI	1	<0.001	
	Ht	1	<0.001	
	CC	1	0.08	

3.2 UAV-derived VIs and their correlation with Yield

The UAV-derived VIs showed varying characteristics of the vegetation and provided contrasting visual indication of nutrient-induced differences in vegetational characteristics, especially in the NOTs (e.g. Fig 5 and 6). The phenological changes between 4WAS and 8WAS growth stages were observable in all the UAV-derived VI images (e.g. Table 2). The NDRE exhibited highest variation across farms, with highest coefficient of variation (CV) of 1.13 in NOT plots at 4WAS, compared to GNDVI which consistently had lowest CV at each growth stage, in both NOT and FMFs. Considering overall data from NOT and FMF, the correlation matrix indicates that none of the VIs had a significant relationship with yield at 4WAS ($r<0.02$, $P>0.1$), however, weak correlation emerged at 8WAS for NDVI and GNDVI ($r\leq0.3$; $P<0.001$). In the NOTs, the VIs and grain yield were weakly correlated at 4WAS (r=0.23 and 0.33 for GNDVI and NDVI, respectively, p<0.001), but this improved at later growth stage, 8WAS (r=0.40 and 0.47 for GNDVI and NDVI, respectively, p<0.001). Contrastingly, in FMF, no meaningful relationship could be established between VIs and grain yield at 4WAS, while the significant relationships at 8WAS were weak ($r\leq0.2$, $p<0.001$).

Preprints (www.preprints.org) | NOT PEER-REVIEWED | Posted: 13 October 2020 doi:10.20944/preprints202010.0264.v1

348 **Table 2:** Descriptive statistics of measured biophysical variables and UAV-derived vegetation indices within multilocation smallholder maize-
349 farms at two growth stages.

		4WAS						8WAS					
	Variable	***min***	***max***	***mean***	***CI (95%)***	***SD***	***CV***	***min***	***max***	***mean***	***CI (95%)***	***SD***	***CV***
NOT + FMF	UNDVI	0.00	0.82	0.42	0.02	0.18	0.43	0.29	0.89	0.77	0.01	0.10	0.13
	NDRE	0.00	0.77	0.29	0.03	0.28	0.98	-0.18	0.82	0.30	0.04	0.31	1.04
	GNDVI	0.24	0.71	0.48	0.01	0.10	0.21	0.39	0.86	0.67	0.01	0.08	0.12
	gNDVI	0.15	0.82	0.42	0.02	0.14	0.34	0.19	0.85	0.68	0.01	0.08	0.12
	Ht (cm)	20.00	105.33	56.91	2.16	17.67	0.31	84.70	314.30	182.12	5.29	43.20	0.24
	CC (%)	0.53	93.59	31.26	2.26	17.32	0.55	7.44	91.67	57.83	1.65	13.51	0.23
	Yld (t/ha)	0.30	9.31	3.18	0.20	1.64	0.52	0.30	9.31	3.18	0.20	1.64	0.52
NOT	UNDVI	0.00	0.76	0.36	0.03	0.17	0.47	0.43	0.89	0.76	0.02	0.10	0.13
	NDRE	0.00	0.75	0.22	0.04	0.25	1.13	-0.17	0.82	0.24	0.05	0.27	1.12
	GNDVI	0.24	0.70	0.45	0.02	0.10	0.21	0.39	0.78	0.68	0.01	0.08	0.12
	gNDVI	0.15	0.82	0.38	0.02	0.12	0.33	0.19	0.85	0.68	0.02	0.09	0.13
	Ht(cm)	24.00	105.33	55.48	3.12	17.98	0.32	92.00	272.67	184.42	6.96	40.10	0.22
	CC (%)	0.53	93.59	33.50	3.36	19.37	0.58	22.92	81.43	57.15	2.16	12.43	0.22
	Yld (t/ha)	0.50	9.31	3.60	0.32	1.83	0.51	0.50	9.31	3.60	0.32	1.83	0.51
FMF	UNDVI	0.15	0.82	0.49	0.03	0.17	0.35	0.29	0.89	0.78	0.02	0.10	0.13
	NDRE	0.03	0.77	0.36	0.05	0.30	0.84	-0.18	0.80	0.36	0.06	0.34	0.95
	GNDVI	0.36	0.71	0.52	0.02	0.09	0.18	0.40	0.86	0.67	0.01	0.09	0.13
	Ht (cm)	20.00	96.70	58.36	3.02	17.31	0.30	84.70	314.30	179.80	8.04	46.16	0.26
	gNDVI	0.15	0.72	0.47	0.03	0.15	0.32	0.45	0.81	0.68	0.01	0.07	0.10
	CC (%)	3.62	63.38	28.32	2.74	13.74	0.49	7.44	91.67	58.53	2.53	14.53	0.25
	Yld (t/ha)	0.30	5.40	2.75	0.23	1.30	0.47	0.30	5.40	2.75	0.23	1.30	0.47

350 CI: Confidence interval ; SD: standard deviation; CV: coefficient of variation; min: minimum value; max: maximum value

Preprints (www.preprints.org) | NOT PEER-REVIEWED | Posted: 13 October 2020 doi:10.20944/preprints202010.0264.v1

351

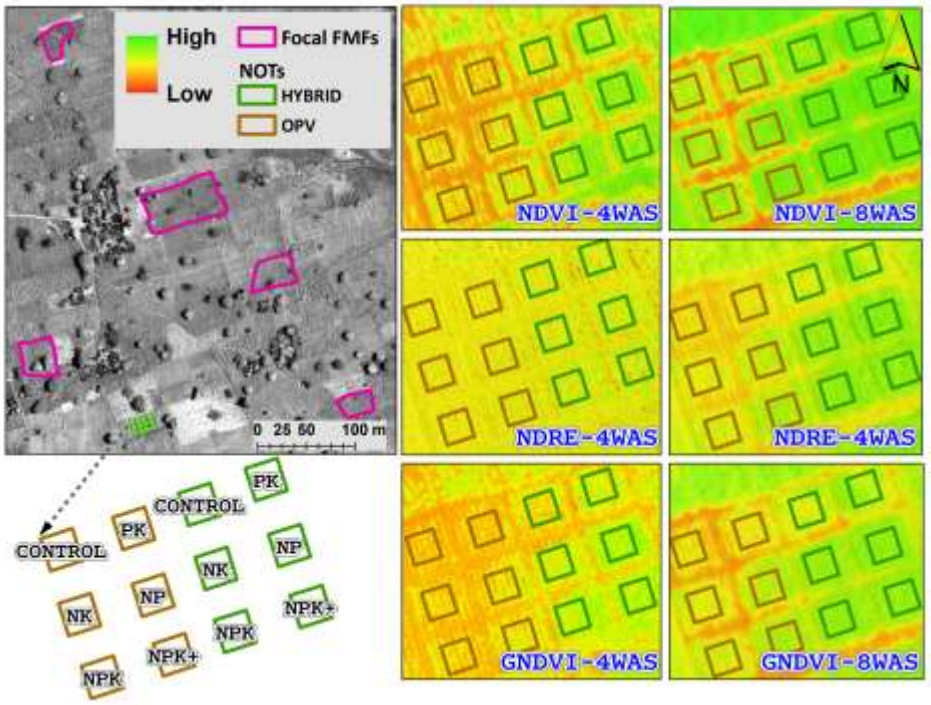

Figure 5: Vegetation indices (VIs) derived from UAV-sensed multispectral imageries, covering maize plots within nutrient omission trials (NOTs) and farmers' fields at Bunkure, Kano. The grey imagery shows red-edge reflectance band acquired at 8 weeks after sowing (WAS) while the colored imageries show the VIs at 4 and 8WAS.

352

Preprints (www.preprints.org) | NOT PEER-REVIEWED | Posted: 13 October 2020 doi:10.20944/preprints202010.0264.v1

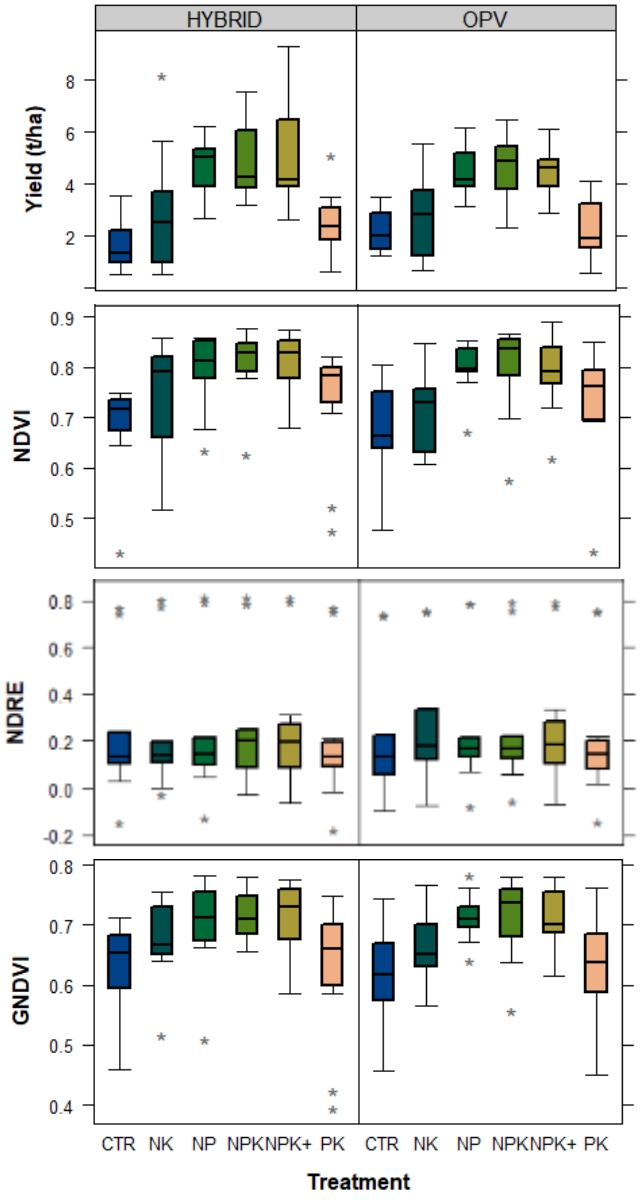

Figure 6: Nutrient-induced variation of UAV-derived vegetation indices (VIs) within multilocational nutrient omission trials (NOTs) in smallholder maize farming systems at 8 weeks after sowing.

*NDVI denotes Normalized difference VI, NDRE is Normalized difference red-edge, and GNDVI is green normalized difference VI.

353

354

Preprints (www.preprints.org) | NOT PEER-REVIEWED | Posted: 13 October 2020 doi:10.20944/preprints202010.0264.v1

355

356 **3.3. Predictability of grain yield variability with(out) biophysical variables**

357 Considering relationship between observed grain yield and each VIs separately, highest explained yield
358 variability at 4WAS and 8WAS growth stages (49% and 54%, respectively) were recorded in NOTs,
359 compared to FMFs where highest yield variability explained was 42% at 4WAS (in the calibration
360 dataset). However, up to 73% of the observed yield variability was explained when the measured Ht
361 variable was separately included in the model, without including the VIs. At the validation stage, the
362 metrics (Tables 3a & b) showed low yield predictability with UAV-derived VIs alone, in both NOTs and
363 FMF. The maximum prediction of yield variability (r=0.56; R^2=0.29) was achieved by fitting the mixed
364 model with GNDVI values from NOTs at 8WAS (Table 3a). There was no meaningful improvement in
365 yield variability that was explained by the VIs after merging datasets from both phenological stages (i.e.
366 4WAS + 8WAS) and analyzing them as time-series data.

367 Comparing the null model with and without the inclusion of each UAV-derived VI as explanatory
368 variable, the accuracy of yield prediction improved, with R^2 increasing from 0.03 (null model) to the
369 highest value of 0.29, based on GNDVI in NOTs. Following the pairwise inclusion of Ht in each prediction
370 model of the UAV-derived VIs, the predictability of grain yield at 4WAS and 8WAS increased significantly
371 in NOTs (Table 3a) but not in FMFs (Table 3b). In NOT, improved predictability of grain yield was seen in
372 NDRE+Ht, with R^2 increasing from non-significant low value (0.03) to a very significant high value (0.63,
373 $p<<0.001$) . Similarly, other VIs showed improved grain yield prediction to attain, with R^2 value peaking
374 at 0.64. The overall yield prediction error, RMSEP mainly decreased after the inclusion of the height
375 parameter (except when 4WAS & 8WAS NDRE data were combined), with maximum change (~79%)
376 associated with NDVI (Table 3a).

377 In contrast to NOTs, the predictability of grain yield with VIs in FMF did not improve meaningfully (at
378 4WAS) or declined (~20% at 8WAS) after the inclusion of Ht variable in each model fit (Table 3b).
379 Similarly, the RMSEP values were stable, hovering around 0.03 – 0.07, at both growth stages assessed.

380

Preprints (www.preprints.org) | NOT PEER-REVIEWED | Posted: 13 October 2020 doi:10.20944/preprints202010.0264.v1

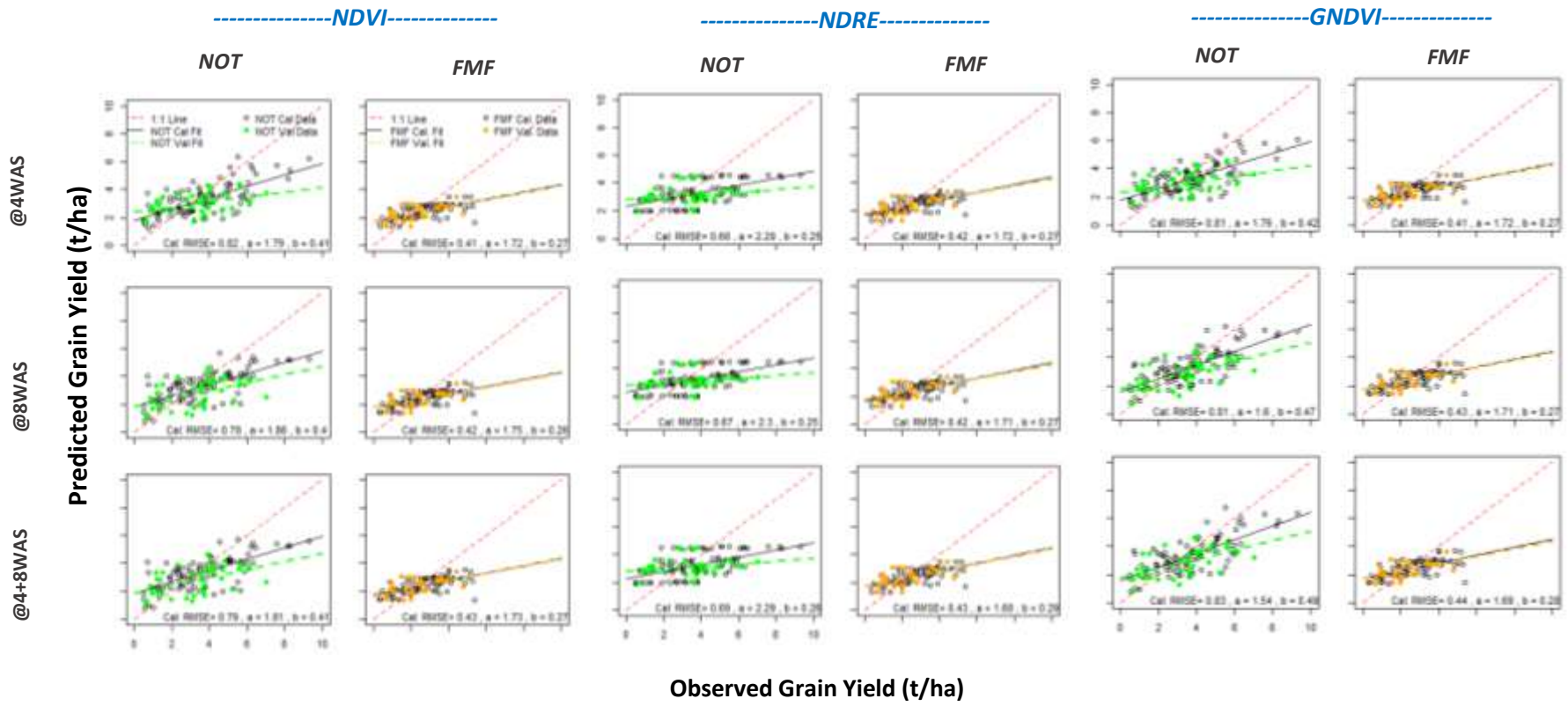

Figure 7a: Relationship between observed and predicted maize grain yield based on fitted linear mixed effect model using UAV-derived Vegetation Indices (VIs) data that was acquired from multilocation smallholder maize farms in Nigeria. NOT=Nutrient Omission Trials; FMF=Farmer managed fields; WAS=Weeks after sowing; a = Intercept; b=slope estimate; *Calibration metrics are shown on the charts and additional validation metrics are presented in Tables 3a&b.

381

382

Preprints (www.preprints.org) | NOT PEER-REVIEWED | Posted: 13 October 2020 doi:10.20944/preprints202010.0264.v1

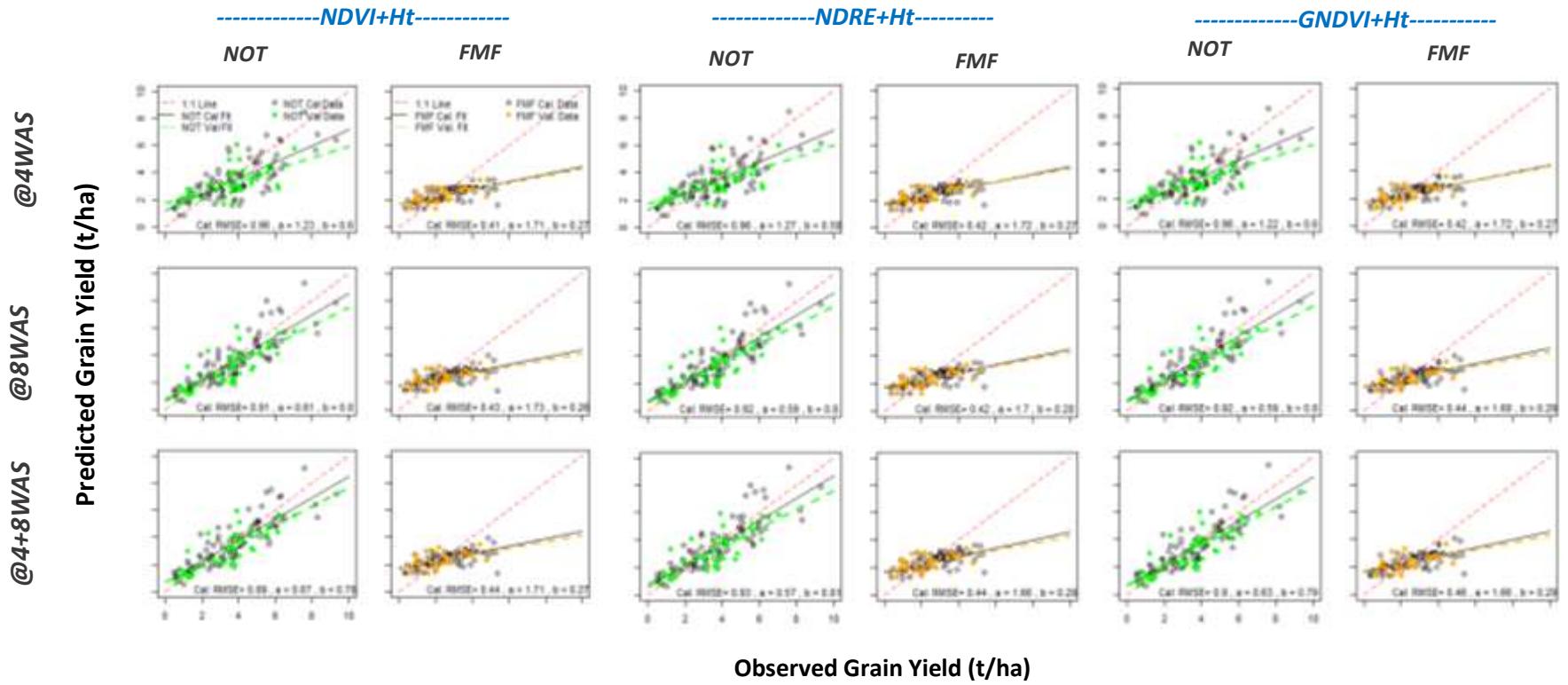

Figure 7b: Relationship between observed and predicted maize grain yield based on fitted linear mixed effect model using and UAV-derived Vegetation Indices (VIs) combined with plant height (Ht) data, from multilocation smallholder maize farms in Nigeria. NOT=Nutrient Omission Trials; FMF=Farmer managed fields; WAS=Weeks after sowing; a = Intercept; b=slope estimate; *Calibration (Cal) metrics are shown on the charts and additional Validation (Val) metrics are presented in Tables 3a&b.

383

384

Preprints (www.preprints.org) | NOT PEER-REVIEWED | Posted: 13 October 2020 doi:10.20944/preprints202010.0264.v1

385 **Table 3a:** Model performance metrics for maize grain yield prediction using UAV-derived vegetation indices (VI), with(out) inclusion of
386 measured biophysical variable, height (Ht) in multilocational Nutrient Omission Trials (NOTs) within farmers' fields.

		No-VI		NDVI		NDRE		GNDVI	
		- Ht‡	*+ Ht*	*- Ht*	*+ Ht*	*- Ht*	*+ Ht*	*- Ht*	*+ Ht*
4WAS	a	-	1.73	2.41	1.75	2.81	1.74	2.35	1.73
	b	-	0.43	0.18	0.41	0.09	0.43	0.19	0.42
	r	-	0.65	0.43	0.63	0.23	0.65	0.43	0.64
	R^2	-	0.41	0.16	0.38	0.03^{ns}	0.40	0.16	0.39
	RMSEP	-	0.21	0.38	0.23	0.29	0.21	0.40	0.23
8WAS	a	-	0.77	1.82	0.77	2.82	0.75	1.80	0.76
	b	-	0.69	0.29	0.68	0.09	0.69	0.33	0.68
	r	-	0.80	0.49	0.79	0.24	0.80	0.56	0.80
	R^2	-	0.62	0.22	0.62	0.03^{ns}	0.63	0.29	0.62
	RMSEP	-	0.30	0.59	0.33	0.29	0.30	0.49	0.32
4+8WAS	a	-	0.80	1.84	0.67	2.8	0.75	1.80	0.69
	b	-	0.69	0.29	0.70	0.09	0.68	0.33	0.71
	r	-	0.80	0.50	0.81	0.23	0.79	0.55	0.81
	R^2	-	0.63	0.23	0.64	0.03^{ns}	0.61	0.29	0.65
	RMSEP	-	0.30	0.57	0.35	0.29	0.32	0.49	0.30

387

388 *ns* denotes non-significance at $\alpha = 0.05$; WAS denotes Weeks After Sowing; a is the model intercept, b is the slope, r is the correlation coefficient,
389 R^2 is the adjusted coefficient of determination, and RMSEP is the root mean square error of prediction. ‡ Metrics of Null yield model without
390 any explanatory variable: a= 2.80; b = 0.09; r = 0.24; $R^2 = 0.03^{ns}$; *RMSEP* = 0.30

391

Preprints (www.preprints.org) | NOT PEER-REVIEWED | Posted: 13 October 2020 doi:10.20944/preprints202010.0264.v1

392 **Table 3b:** Model performance metrics for maize grain yield prediction using UAV-derived vegetation indices (VI), with(out) inclusion of
393 measured biophysical variable, height (Ht) in multilocational smallholder farmers' fields.

		No-VI		NDVI		NDRE		GNDVI	
		- Ht‡	*+ Ht*	*- Ht*	*+ Ht*	*- Ht*	*+ Ht*	*- Ht*	*+ Ht*
4WAS	a	-	1.74	1.73	1.73	1.75	1.75	1.71	1.71
	b	-	0.25	0.26	0.25	0.26	0.26	0.25	0.26
	r	-	0.53	0.53	0.54	0.52	0.53	0.54	0.53
	R^2	-	0.26	0.26	0.26	0.24	0.25	0.26	0.25
	RMSEP	-	0.05	0.05	0.05	0.07	0.06	0.04	0.04
8WAS	a	-	1.75	1.75	1.79	1.75	1.75	1.73	1.74
	b	-	0.25	0.25	0.23	0.26	0.26	0.26	0.25
	r	-	0.53	0.53	0.49	0.52	0.51	0.54	0.51
	R^2	-	0.25	0.25	0.21	0.24	0.23	0.26	0.24
	RMSEP	-	0.04	0.06	0.05	0.07	0.07	0.06	0.04
4+8WAS	a	-	1.74	1.75	1.77	1.72	1.74	1.70	1.71
	b	-	0.25	0.26	0.24	0.27	0.26	0.27	0.26
	r	-	0.53	0.52	0.49	0.53	0.53	0.54	0.50
	R^2	-	0.25	0.24	0.21	0.25	0.25	0.26	0.23
	RMSEP	-	0.04	0.07	0.06	0.07	0.06	0.05	0.03

394

395 *ns* denotes non-significance at $\alpha = 0.05$; WAS denotes Weeks After Sowing; a is the model intercept, b is the slope, r is the correlation coefficient,
396 R^2 is the adjusted coefficient of determination, and RMSEP is the root mean square error of prediction. ‡ Metrics of Null model without any
397 explanatory variable: a= 1.74; b = 0.25; r = 0.53; R^2 = 0.26; RMSEP = 0.05

Preprints (www.preprints.org) | NOT PEER-REVIEWED | Posted: 13 October 2020 doi:10.20944/preprints202010.0264.v1

4.0 Discussion

4.1 Grain yield relationship with measured biophysical variables

In this study, the set-up of NOTs next to farmers field provided important context for the understanding of grain yield gap and predictability in smallholder farming systems. For instance, the attainment of very yield (up to 9.3t/ha) in NOT plots where nutrient limitations are fully addressed, in contrast to control plots where grain yield was as low as 0.49 t/ha, supports the notion that proper soil nutrient management can reduce the existing yield gap within the smallholder farming systems (Giller *et al.*, 2011). Availability of nutrients for plants uptake at various growth stages affects overall plant development, including tallness, greenness, and canopy formation, which are represented by the measured biophysical variables (height, gNDVI, percent canopy, respectively). The significant relationships assessed between observed yield and measured variables (mainly gNDVI and Ht) aligns with previous findings that support selection of relevant proxies for rapid in-season assessment of yield variability (Tittonell *et al*. 2005, Tagarakis and Ketterings, 2017). However, the assessed relationships were weakly expressed ($R^2 \leq 0.17$ and $r \leq 0.42$), in contrast to reported findings where strong relationships were established between maize grain yield and proximally-sensed biophysical variables in Maize farms, with R^2-value typically greater than 0.5 (e.g. Tagarakis and Ketterings, 2017). It should be noted that assessed relationships between yield and proxy variables can be influenced by artefacts of location-dependent soil nutrient conditions and environmental factors, such as short-term drought conditions. Such artefacts can negatively impact the final yield outcome by compromising plant vigor during the reproductive/grain-filling stages (before- and after-8WAS). In the study area, soil nutrient limitations and poor soil management practices are common (Olarinde *et al.*, 2007; Shehu *et al.*, 2018), and we observed that most farmers applied nutrients at early growth stage (mostly by surface dressing or broadcasting) without considering the high potential for rapid nutrient losses due to the sandy textural characteristics of the soil. This prevalent practice may pose implications on the crop performance and predictability of the grain yield based on snapshot spectral information acquired at 2 growth stages. However, further discussions on potential effects of nutrient management practices on yield, based on farmers' resource endowment and preferences, are beyond the scope of this paper.

4.1 Nutrients, not genotype, may influence UAV-derived VIs – Insights from NOT

Based on results derived from the multi-locational NOTs, we noted that the light reflectance signals recorded by the UAV-borne multispectral sensor is more sensitive to nutrient variations than genotype variations in smallholder farmer fields. This provides relevant insight about the potential effect of inherent genotype diversity in smallholder farming systems on wider applicability of UAV across many (and independently managed) farmers fields. Similar to other crops, maize genotypes are often released with intent to improve resilience or tolerance to stress (such as drought and weed) and consequently improve quality and quantity of yield outcomes. In some instances, such improvement may include modification of traits related to leaf morphology and canopy characteristics, to achieve desired response to target stress condition. Despite the expected difference in phenotypic traits of different genotypes (Makanza *et al.*, 2018), the implementation of this study during the wet season, with full control of weed in the experimental plots, may have addressed the major stresses that are likely to compromise

Preprints (www.preprints.org) | NOT PEER-REVIEWED | Posted: 13 October 2020 doi:10.20944/preprints202010.0264.v1

the growth of the OPV genotype in this study. Therefore, it is noteworthy that the variations of soil nutrients exerted dominant effect on the overall yield outcomes for both OPV and Hybrid genotypes, without noticeable contrast. This is further supported by our observed data on percent canopy coverage (not reported) which showed that canopy coverage was similar within the OPV and Hybrid genotype plots, at both growth stages evaluated. Since N and P are the most prevalent soil nutrient deficiencies within the savannah maize-based system of Nigeria (Carsky *et al.*, 1998; Hartmann *et al.*, 2014), the application of appropriate fertilizer likely supported similar leaf formation and ground coverage of maize plant across the plots, without disparity between genotypes.

4.3 In-season grain yield variability prediction with UAV-derived VI: A nuanced outcome

The comparison of grain yield predictability in NOTs versus FMFs unravels often-neglected limitation to the applicability/transferability of agronomic predictive tools from experimental "controlled" conditions to usually "complex" farming systems. Despite the set-up of multilocational NOTs in smallholder farmers field, next to fields that are managed by farmers, we observed a strongly contrasting difference in the potential to predict grain yield based on UAV-derived VIs under both conditions. The differentiated contribution of Ht as an ancillary predictor variable for grain yield, showing high influence in NOTs and negligible/negative influence in FMFs, erodes the expectation that such a variable is universally potent to improve the application of VIs for yield prediction. Rather, an interplay of factors can confound the usefulness of high-resolution UAV-derived VIs, including (amplified) noise that may be generated at the canopy level, especially in smallholder farming systems where canopy formation and structure are usually indeterminate across farms (Giepel *et al.,* 2014; Tittonnel *et al.* 2005).

The grain yield variability explained by the UAV-derived VIs in FMFs (maximum of 42% in calibration and 26% in validation) is lower than reported accuracy from other studies which are based on ground-level proximate-sensing of crop fields, plots, or at point locations (Maresma *et al.*, 2016; Tagarakis and Ketterings, 2017; Tagarakis *et al.*, 2017; Benincasa *et al.*, 2017), and suggests that the application of UAV for in-season yield assessment is limited by issues related to predictability of yield from single (or sparse) time-stamp imageries. Recently, similar findings from complex farming systems in sub-Saharan Africa have been reported (e.g. Wahab *et al.* 2018), where the explained maize yield variability hovered around 40%. Notwithstanding the low predictability of grain yield in farmers' fields, high resolution UAV-imageries are useful to generate agronomically relevant information about crop health and nutrient status. For instance, the UAV-derived VIs distinctly showed major differences between NOTs plots, and to certain extent in the farmers fields (Fig. 5), and this may be useful as a comparative basis for assessment of relative differences in nutrient and overall crop health status in non-uniformly managed smallholder farming systems.

Generally, VIs derived during or close to the reproductive stages have been reported to be more suitable for yield assessment (Schut *et al.* 2018). For instance, around 8WAS, the maize plants are closer to anthesis and plant health at this stage is more likely to determine grain yield outcomes (Ritchie *et al.*, 1993). However, unanticipated environmental stress after the anthesis can negatively impact the grain-filling process, with consequent implication for the final grain yield. The potential to achieve better predictability of grain yield by combining time series imagery-derived VIs (e.g. at 4WAS + 8WAS) deserves further consideration. Our comparison of prediction results from combined time-series data to results from single timestamp (especially at 8WAS) showed negligible or no improvement in the

Preprints (www.preprints.org) | NOT PEER-REVIEWED | Posted: 13 October 2020 doi:10.20944/preprints202010.0264.v1

explained yield variability across farmers' fields. Although this contrasts slightly with the suggestion that time-series UAV imageries may improve yield hindcasting in cropping systems (Schut *et al.* 2018), it aligns with idea that vegetation sensing should be implemented close to the most critical reproductive stage of the target crop (Teal *et al.,* 2006, Maresma *et al.*, 2016, Sakamoto *et al.,* 2014). By implication, the additional costs associated with the acquisition of multiple/time-series imageries (time and resources for flights and analytics) may not be justifiable, given the results of the yield prediction from the time-series data. Rather, targeting the most promising growth stage(s) can potentially be a more suitable and reliable approach.

Although the combination of sparsely measured biophysical variable (mainly Ht) with UAV-derived VIs did not result in any clear gain in the predictability of grain yield in actual farmer-managed fields, Ht stands as a relevant predictor variable, especially in the NOTs. This was shown by the significance of relationship between yield and point-measured canopy Ht ($R^2 \geq 0.62$) in NOT, compared to the null model ($R \geq 0.25$). This suggests that UAV-derived canopy height data may be very relevant for spatially-explicit prediction of grain yield if the mounted sensor is properly calibrated (with ground control references) to provide reliable elevational/surface height (z) data. In agreement with Burke and Lobell (2017), the opportunity to broaden the use of remotely-sensed imageries (including UAV-derived) at a larger scale for rapid yield assessment, especially across complex smallholder farmers' field, may be harnessed with ground data for improved calibration of sensors and models. This is evident under researcher-managed field conditions but results from farmer-managed field conditions seemingly requires further indepth enquiry. We were unable to fully elucidate the other factors that may account yield variability across the Farmer managed fields compared to NOTs due to lack of complete information from farmers. Although the farmers volunteered their farms for data collection and provided basic information on approximate sowing date, they were unavailable and unwilling to document actual tending operations (such as weeding, type and quantity of fertilizer, organic manure application, genotype etc). Future study on complex farming systems should include careful assessment of these potential factors.

5.0 Conclusion

Successful acquisition of quality high-resolution imageries and processing of the agronomically-relevant vegetation indices is an important step towards understanding within- and between-farm spatio-temporal variability of yield and related indicators at field-scale. This study provides further insight into potential use of UAV-derived vegetational indices to assess yield variability for rapid agronomic monitoring and robust decision-support in smallholder farming systems. The weak predictability of maize grain yield variability based on selected indices (NDVI, NDRE, and GNDVI) indicates a lingering gap in UAV application for rapid yield assessment under complex smallholder farming systems, beyond the experimental conditions and large-scale field conditions. By setting up multilocational nutrient omission trials close to several farmers' fields, our findings showed that nutrient, not genotype, significantly explained the observed yield variability. Based on the results obtained from the combination of UAV-derived VIs with the ground-measured and promising biophysical variable (i.e.height), we reckon that the VIs do not provide sufficient basis to reliably predict grain yield. However, a likely advantage associated with the UAV relates to the potential to generate continuous high-resolution canopy height data which may be useful for spatially-explicit relative yield prediction, contingent on accurate calibration. While the demand for in-season prediction of crop yield in smallholder farming systems

remains topical, especially between- and within-fields, further explorations of UAV application should consider and account for potential confounding factors in farmers' fields (such as nutrient application regimes, soil characteristics, and planting density) which can vary between farms and influence canopy formation, light interception, and spectral reflectance at various stages of growth.

Acknowledgement: We thank Dr. A.G. Schut for his very valuable contributions in critiquing the content and analytical approach for this research paper.

Funding: This work was supported by the Bill & Melinda Gates Foundation, Seattle, WA [grant number OPP1113374] under the project Taking Maize Agronomy to Scale in Africa (TAMASA). We thank collaborating partners on this research including Center for Dryland Agriculture, Bayero University Kano (CDA-BUK), International Plant Nutrition Institute (IPNI), and Zonal Advanced Spatial Technology and Analyses Laboratory (ZASTAL) at BUK. Authors wish to declare that no conflict of interest exists in relation to the implementation of this research or in composing this manuscript.

References

Benincasa, P., Antognelli, S., Brunetti, L., Fabbri, C.A., Natale, A., Sartoretti, V. *et al.* 2017. Reliability of NDVI derived by high resolution satellite and UAV compared to in-field Methods for the evaluation of early crop N Status and grain yield in wheat. Expl Agric. doi:10.1017/S0014479717000278.

Burke, M. and Lobell, D.B. 2017. Satellite-based assessment of yield variation and its determinant in smallholder African systems. Proc Natl Acad Sci U S A. 2017 Feb 28;114(9):2189-2194. doi: 10.1073/pnas.1616919114.

Cammarano, D., Fitzgerald G.J., Casa, R., and Basso, B. 2014. Assessing the Robustness of Vegetation Indices to Estimate Wheat N in Mediterranean Environments. Remote Sens. 6, 2827-2844; doi:10.3390/rs6042827

Carletto, C., Jolliffe, D., and Banerjee, R. 2015 From tragedy to renaissance: Improving agricultural data for better policies. J. Dev. Stud. 2015, 51, 133–148.

Carsky, R.J., Nokoe, S., Lagoke, T.O., and Kim, S.K. 1998. Maize yield determinants in farmer-managed trials in the Nigerian northern guinea savanna. Expl Agric. 34:407- 422

Efron, S. 2015. The use of unmanned aerial systems for agriculture in Africa: Can it fly?. Dissertation submitted to Pardee Rand Graduate School. 369p. (Available at: https://www.rand.org/content/dam/rand/pubs/rgs_dissertations/RGSD300/RGSD359/RAND_RGSD359.pdf; Last accessed: 09/07/2017)

Geipel J., Link, J., and Claupein, W. 2014. Combined spectral and spatial modeling of corn yield based on aerial images and crop surface models acquired with an unmanned aircraft system. Remote Sens. 2014:1110335-10355. Doi:10.3390/rs61110335

Giller, K.E., Tittonell, P. Rufino, M.C., van Wijk, M.T., Zingore, S., Mapfumo, P. *et al.* 2011. Communicating complexity: Integrated assessment of trade-offs concerning soil fertility management within African farming systems to support innovation and development.

Gitelson, A.A.; Viña, A.; Rundquist, D.C.; Ciganda, V.; Arkebauer, T.J. Remote estimation of canopy chlorophyll content in crops. Geophys. Res. Lett. 2005, 32, doi:10.1029/2005Gl022688.

Gu, Y., Wylie, B.K., Howard D.M., Phuyal K.P., and Ji, L. 2013. NDVI saturation adjustment: A new approach for improving cropland performance estimates in the Greater Platte River Basin, USA. Ecological Indicators 30 (2013):1-6. Doi: 10.1016/j.ecolind.2013.01.041

Haghighattalab, A., González Pérez, L., Mondal, S., Singh, D., Schinstock, D., Rutkoski, J. *et al.* 2016. Application of unmanned aerial systems for high throughput phenotyping of large wheat breeding nurseries. Plant Methods 12:35. doi: 10.1186/s13007-016-0134-6.

Hall, O. 2016. The challenge of comparing crop imagery over space and time. ICT Update, 82:14-15. Available at http://ictupdate.cta.int; Last Accessed 09/07/2017.

Hartmann, L., Gabriel, M., Zhou, Y, Sponholz, B. and Thiemeyer, H. 2014. Soil Assessment along Toposequences in Rural Northern Nigeria: A Geomedical Approach. Applied and Environmental Soil Science. 2014:628024Hindawi Publishing Corporation. doi:10.1155/2014/628024

578 Hatfield, J.L. and Prueger, J.H . 2010. Value of Using Different Vegetative Indices to Quantify Agricultural
579 Crop Characteristics at Different Growth Stages under Varying Management Practices. Remote Sensing
580 2010, 2, 562-578; doi:10.3390/rs2020562.

581 Herbert, B. 2005. Land use efficiency under maize-based cropping system in Zaria, Nigeria. Journal of
582 Agriculture, Forestry and the Social Sciences 3(1): 114-120.

583 Hijmans, R.J., vanEtten, J., Cheng, J., Mattiuzzi, M., Summer M., Greenber, J.A. *et al.* 2016. Geographic
584 Data Analysis and Modeling: Package Raster. 244 p. [Available at : https://cran.r-
585 project.org/web/packages/raster/raster.pdf; Last Accessed: 02/09/2017)

586 Huete, A., Didan, K., Miura, T., Rodriguez, E.P., Gao, X., and Ferreira, L.G. 2002. Overview of the
587 radiometric and biophysical performance of the MODIS vegetation indices. Remote Sensing of
588 Environment 83:195 – 213.

589 Isla, R., Quílez, D., Valentín, F., Casterad, M.A., Aibar, J., Maturano, M. 2011. Utilización de imágenes
590 aéreas multiespectrales para evaluar la disponibilidad de nitrógeno en maíz (Use of multispectral
591 airbone images to assess nitrogen availability in maize). In Teledetección, Bosques y Cambio Climático;
592 Recondo, C., Pendás, E., Eds.; Asociación Española de Teledetección: Mieres, Spain, 2011; pp. 9–12.

593 Makanza, R., Zaman-Allah, M., Cairns, J.E., Magorokosho, C., Tarekegne, A., Olsen, M., and Prasanna,
594 B.M. 2018. High-Throughput Phenotyping of Canopy Cover and Senescence in Maize Field Trials Using
595 Aerial Digital Canopy Imaging. Remote Sens. 2018, 10, 330; doi:10.3390/rs10020330.

596 Maresma, A, Ariza, M., and Martinez, E., Lloveras, J., and Martinez-Cassanovas, J.A. 2016. Analysis of
597 vegetation indices to determine nitrogen application and yield prediction in maize (*Zea mays* L.) from a
598 standard UAV service. Remote Sensing 8:973 doi:10.3390/rs8120973.

599 Nagy, J.G. and Edun, O. 2002. Assessment of Nigerian Government Fertilizer Policy and Suggested
600 Alternative Market-friendly Policies. Report to International Fertilizer Development Corporation -IFDC.
601 67 p.

602 Nebiker S., Lack N., Abacherli M., and Laderach S. (2016). Light-weight multispectral UAV sensors and
603 their capabilities for predicting grain yield and detecting plant disease. The International Archives of the
604 Photogrammetry, Remote Sensing and Spatial Information Sciences, Vol XLI-B1, 2016. XXIII ISPRS
605 Congress, 12 – 19 July 2016, Prague, Czech Republic.

606 Nguy-Robertson A., Gitelson, A., Peng, Y., Vina, A., Arkebauer, T., and Rundquist, D. 2012. Green leaf
607 area index estimation in maize and soybean: Combining vegetation indices to achieve maximal
608 sensitivity. Agronomy Journal 104(5)1336:1347.

609 Nziguheba, G., Tossah, B., Diels J., Franke, A., Aihou, K., Iwuafor, E., Nwoke, C., Merckx, R. 2009.
610 Assessment of nutrient deficiencies in maize in nutrient omission trials and long-term field experiments
611 in the West African Savanna. Plant Soil. 314:143–157.

612 Olarinde, L.O., Manyong V.M., and Akintole J.O. 2007. Attitudes towards risk among maize farmers in
613 the dry savanna zone of Nigeria: some prospective policies for improving food production. African
614 Journal of Agricultural Research 2(8): 399-408

615 Onuk, E.G., Alimba, J.O., and Kasali, R. 2015. A Comparative Study of Production Efficiencies Under
616 Cowpea-Maize and Groundnut- Millet Intercropping Systems in The North Central Zone, Nigeria. PAT
617 December, 2015; 11 (2): 108-121.

618 Patrignani, A. and Ochsner, T.E., 2015. Canopeo: A powerful new tool for measuring fractional green
619 canopy cover. Agronomy Journal, 107(6), pp.2312-2320.

620 Ritchie S.W., Hanway J.J., and Benson G.O. 1993. How a corn plant develops. Spec. Rep. 48 (revised).
621 Iowa State Univ. of Sc. and Technol. Coop. Ext. Serv., Ames, IA. Available Online at
622 https://s10.lite.msu.edu/res/msu/botonl/b_online/library/maize/www.ag.iastate.edu/departments/agr
623 onomy/corngrows.html#management [Last Accessed, 23/03/2016].

624 Sakamoto, T., Gitelson, A.A., Arkebauer, T.J. Near real-time prediction of US corn yields based on time-
625 series MODIS data. Remote Sens. Environ. 147(19-231)

626 Salami, E., Barrado, C., and Pastor, E. 2014. UAV Flight Experiments Applied to the Remote Sensing of
627 Vegetated Areas. Remote Sensing 6, 11051-11081; doi:10.3390/rs61111051.

628 Schut, A.G.T, Traore, P.C.S., Blaes, X., de By, R.A. 2018. Assessing yield and fertilizer response in
629 heterogeneous smallholder fields with UAVs and satellites. Field Crop Research 221:98-107.

630 Sibley, M.A., Grassini, P., Thomas, N.E., Cassman, K.G., Lobell, D.B. 2013. Testing remote sensing
631 approaches for assessing yield variability among Maize fields. Agron. J. 106:24–32.
632 doi:10.2134/agronj2013.0314

633 Shehu, B.M., Merckx, R., Jibrin, M.J., Kamara, A., and Rurinda, J. 2018. Quantifying Variability in Maize
634 Yield Response to Nutrient Applications in the Northern Nigerian Savanna. Agronomy 8(2)18.

635 Song, Y. 2016. Evaluation of the UAV-Based Multispectral Imagery and Its Application for Crop Intra-Field
636 Nitrogen Monitoring and Yield Prediction in Ontario. Electronic Thesis and Dissertation Repository.
637 Paper 4085. The University of Western Ontario. Canada.

638 Tagarakis, A.C., Ketterings, Q.M., Lyons, S. and Godwin G. 2017. Proximal Sensing to Estimate Yield of
639 Brown Midrib Forage Sorghum. Agronomy, Soils, and Environmental Quality. Agron. J. 109:107–114.
640 doi:10.2134/agronj2016.07.0414

641 Tagarakis, A.C. and Ketterings, Q. M. 2017. In-season estimation of corn yield potential using proximal
642 sensing. Agronomy J. 109:1-8. doi: 10.2134/agronj2016.12.0732

643 Teal, R.K., Tubana, B., Girma, K., Freeman, K.W., Arnall, D.B., Walsh, O., and Raun, W.R. 2006. In-season
644 prediction of corn grain yield potential using normalized difference vegetation index. Agron. J. 98:1488–
645 1494. doi:10.2134/agronj2006.0103

646 Tittonell, P., Vanlauwe, B., Leffelaar, P.A., and Giller, K.E. 2005. Estimating Yields of Tropical Maize
647 Genotypes from non-destructive, on-farm plant morphological measurements. Agriculture, Ecosystems,
648 and Environment 105:213-220. doi:10.1016/j.agee.2004.04.002.

649 Tucker, C. J. 1979.Red and photographic infrared linear combinations for monitoring vegetation. Remote
650 Sensing of Environments 8:127-150.

651 Vanlauwe, B., Coe, R., and Giller, K.E. 2015. Beyond Averages: New Approaches to Understand
652 Heterogeneity and Risk of Technology Success or Failure in Smallholder Farming. Expl Agric. pp1-23.
653 Cambridge University Press 2016. doi:10.1017/S0014479716000193

654 Vega, F.A., Ramirez, F.C., Saiz, M.P., Rosua, F.O. 2015. Multi-temporal imaging using an unmanned aerial
655 vehicle for monitoring of sunflower crop. Biosystems Engineering 132:19-27.

656 Viña, A., Gitelson A.A., Nguy-Robertson A.L., and Peng Y. 2011. Comparison of different vegetation
657 indices for the remote assessment of green leaf area index of crops. Remote Sensing of the
658 Environment. doi:10.1016/j.rse.2011.08.010

659 Wahab, I., Hall. O., Jirstrom M. 2018. Remote Sensing of Yields: Application of UAV Imagery-Derived
660 NDVI for Estimating Maize Vigor and Yields in Complex Farming Systems in Sub-Saharan Africa. Drones
661 2:28, 1-16. doi:10.3390/drones2030028

662 Watanabe, K., Guo, W., Arai, K., Takanashi, H., Kajiya-Kanegae, H., Kobayashi, M. *et al.* 2017. High-
663 Throughput Phenotyping of Sorghum Plant Height Using an Unmanned Aerial Vehicle and Its Application
664 to Genomic Prediction Modeling. Frontiers. Plant Sci. 8:421. doi: 10.3389/fpls.2017.00421.

665 Xue, J. and Sue, B. 2017. Significant Remote Sensing Vegetation Indices: A Review of Developments and
666 Applications. Journal of Sensors. Volume 2017, Article ID: 1353691.
667 https://doi.org/10.1155/2017/1353691

668 Yang, G., Liu, J., Zhao, C., Li, Z., Huang, Y., Yu, H., *et al.* 2017. Unmanned aerial vehicle remote sensing
669 for field-based crop phenotyping: Current status and perspectives. Front Plan Sci 8:1111. doi:
670 10.3389/fpls.2017.01111

671 Zhang, C., Walters, D., Kovacs, J.M. 2014. Applications of Low Altitude Remote Sensing in Agriculture
672 upon Farmers' Requests– A Case Study in Northeastern Ontario, Canada. PLoS ONE 9(11): e112894.
673 doi:10.1371/journal.pone.011289

674